Received: 27 June 2019 | Revised: 3 December 2019 | Accepted: 3 December 2019

DOI: 10.1002/sia.6739

SPECIAL ISSUE ARTICLE

SURFACE and INTERFACE ANALYSIS WILEY

Chemical states of ppm cerium in steel by ToF-SIMS analysis

Chunli Dai | Fei Guo | Pei Wang | Dianzhong Li | Lei Zhang

Shenyang National Laboratory for Materials Science, Institute of Metal Research, Chinese Academy of Sciences, Shenyang, China

Correspondence
Lei Zhang, Shenyang National Laboratory for Materials Science, Institute of Metal Research, Chinese Academy of Science, 72 Wenhua Road, Shenyang 110016, China.
Email: lzhang@imr.ac.cn

Funding information
Innovation Promotion Association, Chinese Academy of Sciences, Grant/Award Number: 2013126; National Natural Science Foundation, Grant/Award Number: U1708252

Time-of-flight secondary ion mass spectrometry (ToF-SIMS) was employed for an analysis of the rare earth element Ce in pure iron and steel. Secondary ion images showed that the amount of the segregation of Ce and its oxides was much less as the concentration of Ce decreased to about 11 ppm in the pure iron. In terms of depth profiling from the surface to the matrix, variation of the CeO^+/Ce^+ ratio in a Ce oxides sample and a pure Ce sample exhibited difference between oxidized state and metallic state. It was demonstrated that metallic Ce was presented when the ratio of CeO^+/Ce^+ decreased to approximately 2 and even smaller. Oxygen content with concentration of tens of ppm may influence the ratio obviously. Such ToF-SIMS analysis was also feasible to discern the states of cerium in a Q345E steel with concentration in ppm level.

KEYWORDS
chemical states, oxides, rare earth, solid solution, steel, ToF-SIMS

1 | INTRODUCTION

Rare earth (RE) elements are broadly utilized in functional materials, RE permanent magnetic materials,[1,2] luminescent materials,[3] and hydrogen storage materials.[4,5] For structural materials, RE elements play an important role in purification,[6] heterogeneous nucleating agents,[7-9] and modifiers of nonmetallic inclusions.[10-16] Moreover, they have been found to strengthen the grain boundary and suppress the crack propagation with more impact energy absorption.[17] Many studies have confirmed that an extremely small amount of RE addition can change the phase transformation temperature points during heating or cooling without an obvious modification of the composition. Consequently, the microstructure of the materials at room temperature might vary as a result of the RE addition. As an example, it influences the dissolution and precipitation process of the internal carbides of steel.[18-24]

Characterization of RE elements is of critical importance for their effective usage in alloys and control of their influence on the microstructures of the materials formed. The different forms of RE elements in steel can be roughly divided into two categories, namely, a combination or a solid solution. It has been extensively reported that RE elements are easily combined with inclusions in steel. Although solid solutions have recently attracted greater attention,[25,26] they require effective analytic tools for characterization and evaluation. Nonwater electrolysis has been proven to be a feasible approach for RE identification in carbon-containing steel.[17] However, this is not a solid chemical analysis method for modern steel containing extremely large amounts of solute elements through alloying. For iron-based materials, there are two main forms of RE elements in the matrix, one is the combination of RE elements found in oxides and sulfides, and the other is RE elements dissolved in the grains or grain boundaries. Nevertheless, the total amount of RE elements can only be obtained through traditional detection methods such as inductively coupled plasma mass spectrometry, and the distribution or chemical state of the RE elements cannot be figured out in detail. Although electron probe microanalysis and X-ray photoelectron spectroscopy can generally be used to characterize the state of RE in solid, they are difficult to probe RE of concentration in ppm range because of their detection limits at one-tenth of 1%.

Time-of-flight secondary ion mass spectrometry (ToF-SIMS) has been widely used for the analysis of trace elements in solid materials, particularly semiconductor materials, thin-film materials, and even composite materials. The bombardment of the sample surface by a primary ion beam can produce charged monoatomic or polyatomic particles for a mass spectrum analysis using a time-of-flight detector. A high mass resolution and ppm concentration detection limit for element information combined with a depth profiling capability makes ToF-SIMS a suitable analysis tool for an accurate characterization of

the RE elements in a solid material within a depth of a few micrometers on top of the surface. It is necessary to take additional aspects into account to distinguish the oxidation state of RE in iron or steel. In this work, Ce oxides were detected in two modalities: Ce^+ and CeO^+. However, the Ce present in even a solid solution might also be reacted to form Ce^+ and CeO^+ owing to the solute oxygen present in the matrix.

To determine whether the Ce has oxidized even in pure iron or steel, ToF-SIMS is employed to establish a correlation between the intensity of each characteristic ion obtained and the chemical states of the corresponding elements through a relative intensity analysis. In the present study, emphasis was placed on the advantages of ToF-SIMS in characterizing the RE distribution and the feasibility of ToF-SIMS in detecting the content of solid dissolved RE elements in pure iron and steel.

2 | EXPERIMENTAL

As-cast iron with various amounts of La-Ce mixed RE elements within a range of tens of ppm to a few percentages in weight was created through arc melting. The resulting Ce concentration in the samples was measured through inductively coupled plasma optical emission spectroscopy with accuracy better than 5 ppm. High-purity stocks of La and Ce were used as an additive for the arc melting. Both of these RE elements have very similar properties for alloying. For comparison, fully oxidized RE elements embedded in the pure iron matrix were also prepared using powder metallurgy. High-purity micron-grade iron powder mixed with high-purity CeO_2 of a 300 ppm equivalent weight was processed using spark plasma sintering (SPS). Arc-melting and SPS samples were machined to a size of 11 mm × 11 mm × 7 mm and then finely polished for the ToF-SIMS experiments. The surface layer with deformations induced through residual stresses was removed using electrolytic polishing.

Analysis was conducted using a ToF-SIMS V from ION-TOF GmbH. ToF-SIMS images were acquired using 30-keV Bi^+ in a 300 × 300 μm^2 area with a lateral resolution of 220 nm. The depth profiling for an arc-melting sample containing approximately 200 ppm Ce and an SPS sample of a 300 ppm equivalent weight of Ce in pure iron was carried out by alternately applying a ToF-SIMS analysis and Cs sputtering at 2 keV. Because of the lower count intensity for samples with a Ce concentration of lower than 100 ppm, before the ToF-SIMS analysis, the surface was first sputtered using a primary Bi^+ ion beam under the direct-current (DC) mode to remove absorptions on the surface and some of the layers on top. The effective data acquisition process began when the sample surface was stripped off to a depth of approximately 50 nm. A primary Bi^+ ion beam with a voltage of 30 keV and a current of 1.0 pA was used for the SIMS analysis. After three scans on a 500 × 500 μm^2 area under Bi^+ DC mode, the mass spectrum was collected for 300 seconds using a 128 pixel × 128 pixel area under a vacuum of 1.0×10^{-9} mbar. Five areas were analyzed for each specimen. The intensities of the Ce^+ and CeO^+ ions were then normalized based on the total intensity to eliminate the effects of the ion source instability. The intensity values of these five areas were averaged for better statistics. All original data for the ions ratio calculation are supplied in the Supporting Information.

3 | RESULTS AND DISCUSSION

Figure 1 clearly shows the distributions of the Ce^+ and CeO^+ signals through the ToF-SIMS images for two arc-melting samples. The difference between the different Ce contents was obvious. For a sample with a much higher Ce concentration of 2.84 wt%, both the Ce^+ and CeO^+ signals have two types of morphology, a network formed along the boundaries and high-density bright spots embedded in the matrix with a feature size in micrometers, as shown in Figure 1A,B. These two features of morphology correlate extremely well for the Ce^+ and CeO^+ signals. It is clear that they might be generated from a similar component or structure in the matrix investigated. Because RE elements are considered a good deoxidant element for steel making, they are very easily combined with oxygen and form RE oxides or a complex oxide compound. Thus, the boundary network and scattered spot of CeO^+ in the ToF-SIMS images indicate that plenty of RE oxide compounds are formed during arc-melting for a large amount of RE addition of several percentage points in weight. For the sample with a lower Ce concentration of 11 ppm, in contrast, the Ce^+ signal was rather uniformly distributed and few CeO^+ bright spots scattered over the area were scanned, as shown in Figure 1C,D. However, the total count of the Ce^+ ions in this sample was one order of magnitude lower than that of the higher content Ce sample. Except those detected Ce^+ ions that are related to the CeO^+ spot that might originate in the oxide compound containing Ce, most of the evenly distributed Ce^+ signal was generated from the iron matrix. It implies that a small portion of the Ce might be solute in the iron matrix. This means the Ce in the form of an oxide compound is the main source generating the CeO^+ signals; other than that, the Ce could be a metallic state as in solid solution. The two samples exhibited extreme cases in terms of the Ce content with higher and lower concentrations as based on the ToF-SIMS imaging technique. However, limited by the resolution, an imaging technique is not a reliable method to justify the chemical state of oxides state or metallic state for a much broader range of RE concentration at the ppm level.

To distinguish the solid solution from the oxide compound, a quantitative analysis must be explored. The ratio of CeO^+/Ce^+ was proposed as a sign to indicate the extent of oxidation, no matter what the Ce is in the state of fully oxides, pure metallic state as in solid solution or mixed.

Powder metallurgy samples of an iron and oxidized RE mixture prepared using SPS were applied to investigate the characteristic ratio of CeO^+/Ce^+ when all RE elements were thought to exist as oxide compounds. Sequential scanning in ToF-SIMS DC mode was used to evaluate the ratio of CeO^+/Ce^+ with an increase in depth. The ion intensity levels obtained at different scanning times are shown in Figure 2a (from Figure S1a). In the early stages of scanning within the same area, owing to the complex condition on top of the sample

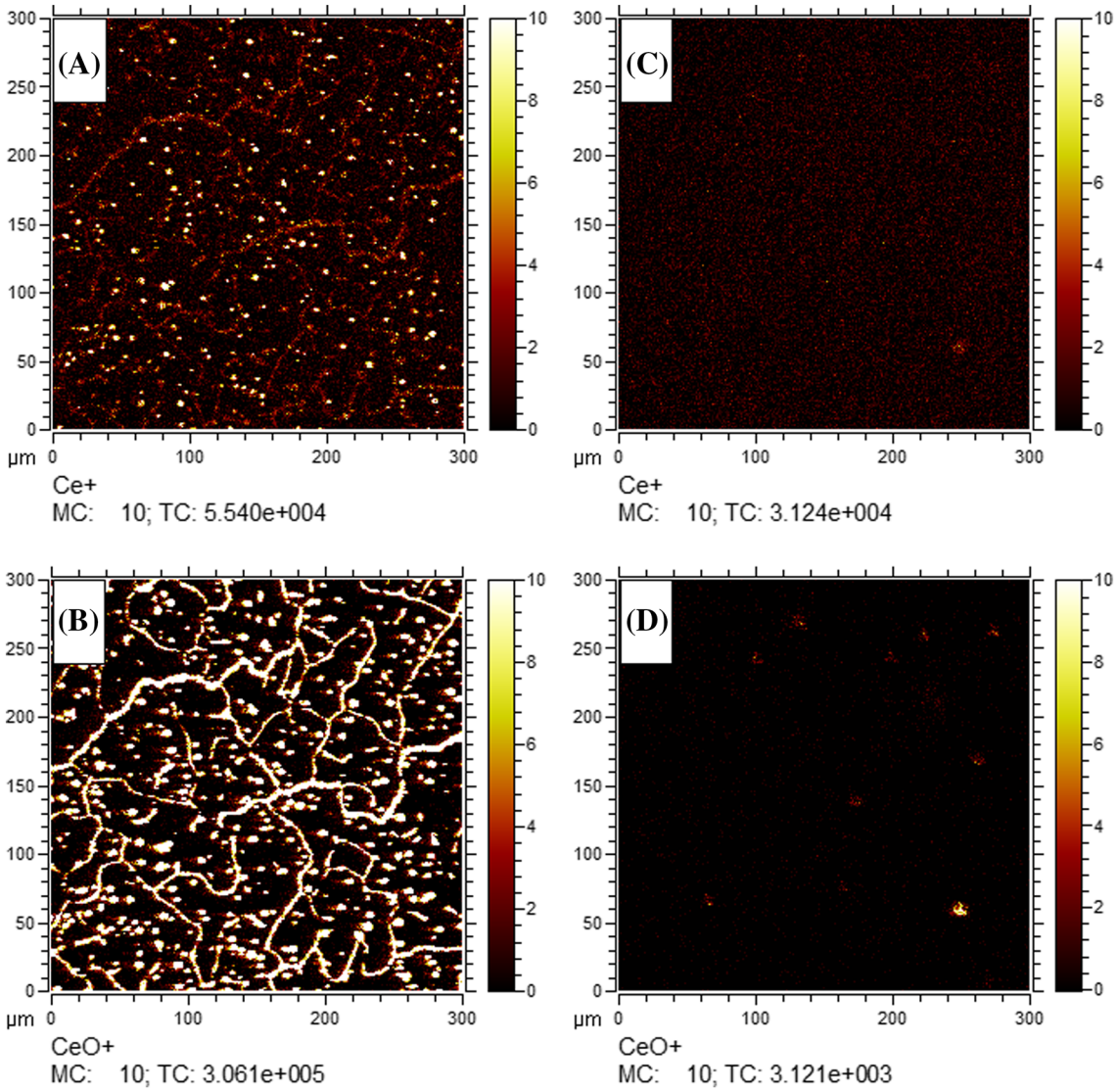

FIGURE 1 ToF-SIMS images of Ce^+ and CeO^+ in arc melted sample with different Ce concentrations of 2.84 wt% (A,B) and 11 ppm (C,D)

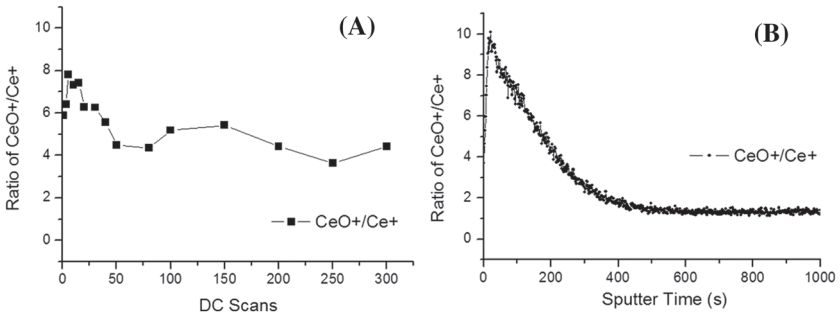

FIGURE 2 Depth profile of CeO^+/Ce^+ ratio in two samples: A, powder metallurgy mixture of iron and 300 ppm CeO_2 with the number of DC scans, and B, bulk pure Ce with 100 ppm oxygen based on the sputtering time

surface, the ratio was varied from 6 to 8. As the depth increases with the number of DC scans, the ratio started to decrease from the maximum value of 8 and was gradually stabilized at approximately 4 after 200 scans. In the case of Ce oxides and an iron mixture, it is persuasive to regard a CeO^+/Ce^+ ratio of 4 as an eigenvalue corresponding to the fully oxidized states of the Ce in the iron matrix.

A naturally formed gradient of oxidation presented on the pure Ce sample surface, which is a good object for investigation in a comparison of the Ce oxidation state between the surface and matrix. As shown in Figure 2B for the depth profiling of the bulk Ce sample with 100 ppm oxygen (from Figure S1b), the change in CeO^+/Ce^+ ratio at depth with an oxidation gradient clearly showed a change in value

between the oxide layer and matrix. The ratio was increased from approximately 4 to 10 around the outmost surface layers. The maximal ratio in the sample was even larger than in the SPS sample, which may be attributed to the enhanced CeO^+ ionization for unstable oxides compared with the full oxidation of Ce. The ratio profile deceased smoothly from 10 to 2 and then became rather stable at about 1.5 after sputtering for 600 seconds. It slowly decreased to 0.8 with a further and deeper sputtering during 10 000 seconds. This indicated that metallic Ce in the matrix might be obviously presented when the ratio was less than 2.

The chemical state of the fully oxidized Ce compound agrees reasonably well in the SPS sample and the oxidation gradient on the surface of the pure bulk Ce sample where the ratio was larger than 4. Nevertheless, it was still difficult to deduce the ratio for a Ce solid solution in terms of the smaller ratio 2 from the pure Ce sample. Dissolved oxygen in the matrix cannot be ignored and might combine with the charged Ce ions to form CeO^+ because of the ionization process. An experimental comparison of varying oxygen contents with a similar Ce concentration at the ppm level encountered difficulty in the sample preparation. Because the RE mixture additive in iron during arc melting significantly affected the oxygen concentration of the sample, and the resulting concentration of RE in the sample was also difficult to control. But the solute oxygen in the matrix indeed affects the ratio, which can be deduced from the depth profile of the FeO^+/Fe^+ ratio in the pure iron samples, as shown in Figure 3 (from Figure S2a and S2c). Two pure iron samples with a small difference in oxygen content, namely, 20 and 50 ppm, were investigated. The stable ratio of FeO^+/Fe^+ away from the surface was close to 0.2 for the 20 ppm oxygen and approximately 0.5 for the 50 ppm oxygen. This indicated that the ratio was extremely sensitive to the solute oxygen in the matrix even the oxygen concentration at ppm level. It was also implied that the solute oxygen might be helpful for the MO^+ ionization in a metallic matrix (M).

The previous results of the Ce chemical state whether under oxidation or metallic state were derived. Other ingredients or constitutes

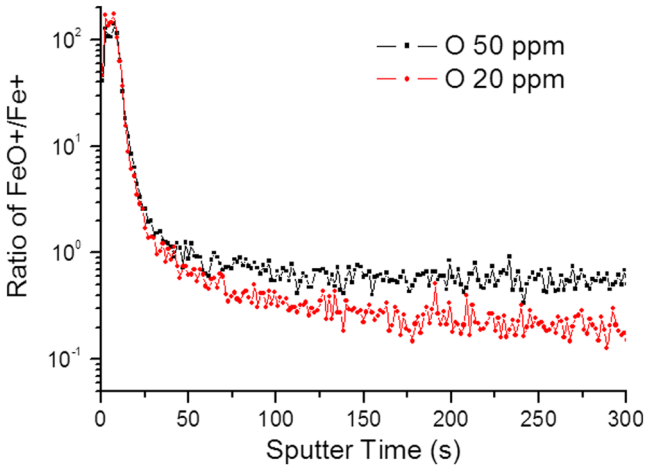

FIGURE 3 Depth profiles of FeO^+/Fe^+ ratio for pure iron samples containing 50 and 2 ppm oxygen

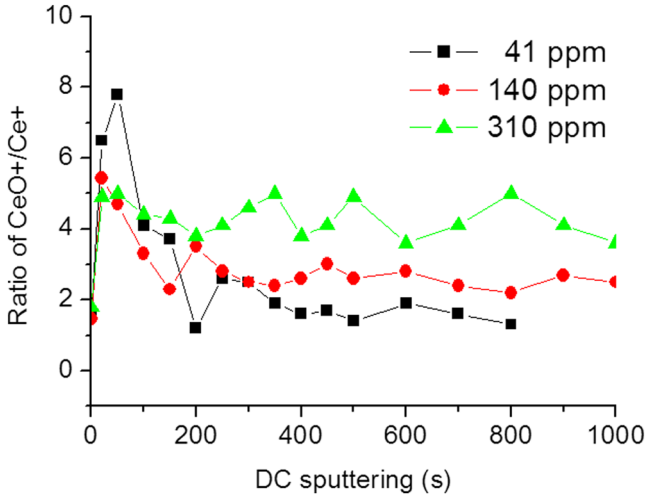

FIGURE 4 CeO^+/Ce^+ ratio in Q345E steel with Ce content of 41, 140, and 310 ppm

might change the matrix and affect the ion generation owing to the matrix effect for the ToF-SIMS analysis. The widely used Q345E is a low-carbon steel with a small amount of alloying element with Si and Mn solutes. The La-Ce RE additive in Q345E steel with different contents was also investigated. The samples were prepared by the arc-melting with less oxygen content at about 10 ppm. Figure 4 shows the ratio of CeO^+/Ce^+ at varying Ce concentrations of 41 (from Table S1), 140, and 310 ppm. The results also showed that the ratio changes at depth with sputtering in DC mode. The profiles of these samples show similar features, as indicated in Figure 4, where a transient region from the surface to the bulk matrix can be observed at a DC sputtering time of approximately 50 to 200 seconds. In the sample with a Ce concentration of 41 ppm, the ratio reaches a maximum value of 8 and decreases to a stable value of approximately 1.5. However, the ratio oscillates at approximately 4 to 5 for the sample with a higher Ce concentration of 310 ppm. The profile of the sample with the middle Ce concentration of 140 ppm was placed between the other two profiles. The previous conclusion of the critical ratio value was still viable to explain the state of Ce in these samples. The oxide compound with Ce was dominant in the sample with a higher Ce concentration, and the solid solution state could be distinguished as in the lower Ce concentration of 41 ppm. The matrix effects on the ratio analysis from the carbon and alloy element solutes in steel were not obvious.

4 | CONCLUSIONS

An ion ratio analysis in terms of the ToF-SIMS depth profiling data can provide viable and informative results to determine a solid solution or oxidation state for RE elements. The RE element Ce in iron and steel was observed to be segregated at the grain boundary or in dispersed oxides, respectively, although a very small amount of Ce may dissolve into the bulk lattice. The change in CeO^+/Ce^+ ratio along depth for the Ce oxides embedded in the iron matrix or the natural

oxidation gradient in the pure Ce indicated that the ratio for the Ce oxides was larger than 4, metallic Ce as in solid solution might be presented when the ratio was less than 2. However, the concentration of dissolved oxygen in the bulk matrix can influence the CeO^+/Ce^+ ratio, which can be deduced from the depth profile of the FeO^+/Fe^+ ratio in the pure iron sample. In the Q345E matrix, the carbon and alloy element solutes had little effect on the CeO^+/Ce^+ ratio. Such ToF-SIMS analysis was also feasible to discern distribution and chemical states of other RE content in steel with concentration in ppm level.

ACKNOWLEDGMENTS

This work was supported by the National Natural Science Foundation (grant no. U1708252) and Youth Innovation Promotion Association, Chinese Academy of Sciences (grant no. 2013126).

ORCID

Lei Zhang https://orcid.org/0000-0003-2530-7853

REFERENCES

1. Sugimoto S. Current status and recent topics of rare-earth permanent magnets. *J Physics D: Applied Physice*. 2011;44(11):064001.
2. Dent PC. Rare earth elements and permanent magnets (invited). *J Appl Phys*. 2012;111(7):07A721.
3. Zhang X, Zhang W, Li Y, Li C. Hybrid luminescent materials of graphene oxide and rare-earth complexes with stronger luminescence intensity and better thermal stability. *Dyes and Pigments*. 2017;140:150-156.
4. Wang L, Ma CA, Mao X, Sheng J, Bai F, Tang F. Rare earth hydrogen storage alloy used in borohydride fuel cells. *Electrochem Commun*. 2005;7(12):1477-1481.
5. Louis Schlapbach AZ. Hydrogen-storage materials for mobile applications. *Nature*. 2001;414(15):353-358.
6. Xiaowei Huang ZL, Wang L, Feng Z. Technology development for rare earth cleaner hydrometallurgy in China.pdf. *Rare Metals*. 2015;34(4):215-222.
7. Liang Y, Yi Y, Long S, Tan Q. Effect of rare earth elements on isothermal transformation kinetics in Si-Mn-Mo bainite steels. *J Mat Eng Perform*. 2014;23(12):4251-4258.
8. Minggui QU, Zhenhua WA, Hui LI, Zhiqing LV, Shuhua SU, Wantang F. Effects of mischmetal addition on phase transformation and as-cast microstructure characteristics of M2 high-speed steel. *J Rare Earths*. 2013;31(6):628-633.
9. Feifei H, Bo L, Da L, et al. Effects of rare earth oxide on hardfacing metal microstructure of medium carbon steel and its refinement mechanism. *J Rare Earths*. 2011;29(6):609-613.
10. Adabavazeh Z, Hwang WS, Su YH. Effect of adding cerium on microstructure and morphology of Ce-based inclusions formed in low-carbon steel. *Sci Rep*. 2017;7(10):46503.
11. Opiela M, Grajcar A. Modification of non-metallic inclusions by rare-earth elements in microalloyed steels. *Archives of Foundry Eng*. 2012;12(2):129-134.
12. Maloney JL, Garrison WM. The effect of sulfide type on the fracture behavior of HY180 steel. *Acta Mater*. 2005;53(2):533-551.
13. Ma Qiqi WC, Guoguang C, Fengwei L. Characteristic and formation mechanism of inclusions in 2205 duplex stainless steel containing rare earth elements. *Materials Today: Proceedings*. 2015;2S:S300–S305.
14. Liu C, Revilla RI, Liu Z, Zhang D, Li X, Terryn H. Effect of inclusions modified by rare earth elements (Ce, La) on localized marine corrosion in Q460NH weathering steel. *Corros Sci*. 2017;129:82-90.
15. Park JH. Effect of inclusions on the solidification structures of ferritic stainless steel: computational and experimental study of inclusion evolution. *Calphad*. 2011;35(4):455-462.
16. Wen B, Song B, Pan N, Shu QF, Hu XJ, Mao JH. Influence of Ce on characteristics of inclusions and microstructure of pure iron. *J Iron Steel Res Int*. 2011;18(2):38-44.
17. Lin Qin YW, Shuanlu L, Zongsen Y. Rare earth dissolved in solid solution of steel and its effect on microstructure. *J Chinese Rare Earth Soc*. 1989;7(2):55-60.
18. Yan H, Hu Y, Zhao D. The influence of rare earth elements on phase transformation in 25Mn steel during continuous heating. *Metallurgical and Materials Transactions A*. 2018;49(11):5271-5276.
19. Liu H-L, Liu C-J, Jiang M-F. Effect of rare earths on impact toughness of a low-carbon steel. *Materials & Design*. 2012;33:306-312.
20. Chen X, Li Y. Fracture toughness improvement of austempered high silicon steel by titanium, vanadium and rare earth elements modification. *Mater Sci Eng A*. 2007;444(1-2):298-305.
21. Xiang Yong CZ, Xiang W, Zhongjia W. Influence of Ce on microstructure and properties of high-carbon high-boron steel. *Rare Met Mater Eng*. 2015;44:1335-1339.
22. Ahn J-H, Jung HD, Im JH, Jung KH, Moon BM. Influence of the addition of gadolinium on the microstructure and mechanical properties of duplex stainless steel. *Mater Sci Eng A*. 2016;658:255-262.
23. Zhang Shaohua YY, Shebin W, Hao L. New study concerning development of application of rare earth metals in steels. *J Rare Earths*. 2017;35(5):518-524.
24. Wang L-M, Lin Q, Yue LJ, Liu L, Guo F, Wang FM. Study of application of rare earth elements in advanced low alloy steels. *J Alloys Compd*. 2008;451(1-2):534-537.
25. Gao L, Chen RS, Han EH. Effects of rare-earth elements Gd and Y on the solid solution strengthening of Mg alloys. *J Alloys Compd*. 2009;481(1-2):379-384.
26. Ji Y, Zhang M-X, Ren H. Roles of Lanthanum and cerium in grain refinement of steels during solidification. *Metals*. 2018;8(11):884.

SUPPORTING INFORMATION

Additional supporting information may be found online in the Supporting Information section at the end of this article.

How to cite this article: Dai C, Guo F, Wang P, Li D, Zhang L. Chemical states of ppm cerium in steel by ToF-SIMS analysis. *Surf Interface Anal*. 2020;52:301–305. https://doi.org/10.1002/sia.6739